

# Long-range transport of ozone, carbon monoxide, and aerosols to the NE Pacific troposphere during the summer of 2003: Observations of smoke plumes from Asian boreal fires

Isaac T. Bertschi and Daniel A. Jaffe<sup>1</sup>

Department of Interdisciplinary Arts and Sciences, University of Washington, Bothell, Washington, USA

Received 16 June 2004; revised 15 October 2004; accepted 16 December 2004; published 15 March 2005.

[1] Using a small aircraft, we conducted nine flights from 27 May through 5 August 2003 to collect vertical profiles of ozone, carbon monoxide, and total aerosol scattering in the 0–6 km column off the coast of Washington State. During 27 May, 2 June, and 5 August 2003 we observed air masses containing highly correlated and well-defined layers of O<sub>3</sub>, CO, and aerosol enhancements within the 0–6 km column. The largest of these pollution episodes, or “events,” occurred on 2 June 2003 when O<sub>3</sub> and CO mixing ratios exceeded 100 and 220 ppbv, respectively. A suite of meteorological data indicated that these polluted layers were not due to local sources. NOAA Hysplit backward trajectories indicate that the polluted air masses originated from a vast region in Asia bounded by 35°–70°N and 70°–170°E and transited the Pacific Ocean at middle and upper latitudes to North America in 7–10 days. Satellite data and global aerosol transport models suggest that Siberian boreal fire emissions were the primary source of the three events. Our observations indicate that ozone and aerosol scattering enhancement ratios, O<sub>3</sub>/CO and  $\sigma_{sp}(550\text{ nm})/\text{CO}$  ERs, during these episodes were relatively large and varied from 0.15 to 0.84 ppbv ppbv<sup>-1</sup> and 0.24 to 1.24 Mm<sup>-1</sup> ppbv<sup>-1</sup>, respectively. These observations coupled with ground-based measurements suggest that under certain circumstances, Siberian smoke was transported to the surface and had a significant influence on regional air quality in western Washington State. Notably, the 2 June event coincides with a period when O<sub>3</sub> concentrations exceeded the U.S. Environmental Protection Agency 8-hour standard (>84 ppbv) in Enumclaw, Washington, and the 5 August event corresponded with air quality degradation in Seattle, Washington, when 24-hour average fine particle (PM<sub>2.5</sub>) concentrations exceeded 18  $\mu\text{g m}^{-3}$  during the first week of August.

**Citation:** Bertschi, I. T., and D. A. Jaffe (2005), Long-range transport of ozone, carbon monoxide, and aerosols to the NE Pacific troposphere during the summer of 2003: Observations of smoke plumes from Asian boreal fires, *J. Geophys. Res.*, *110*, D05303, doi:10.1029/2004JD005135.

## 1. Introduction

[2] Since the mid-1980s, several ground-based and airborne studies have investigated the long-range transport (LRT) of trace gas and particle emissions from Eurasia to the northeast Pacific and North America [Andreae et al., 1988; Kritz et al., 1990; Parrish et al., 1992; Husar et al., 2001; Jaffe et al., 1999, 2001, 2003a, 2003b, 2004; Kotchenruther et al., 2001a; Price et al., 2003; Weiss-Penzias et al., 2003, 2004; Bertschi et al., 2004]. It has been well-established that air masses transported from the Asian boundary layer often contain a suite of trace gases and particles, including

ozone (O<sub>3</sub>), carbon monoxide (CO), nitrogen oxides (NO<sub>x</sub> = NO + NO<sub>2</sub>), volatile organic compounds (VOCs), soot and/or mineral dust [Bey et al., 2001; Kotchenruther et al., 2001a; VanCuren, 2003; Jaffe et al., 2003a, 2003b; Price et al., 2003; Jacob et al., 2003; Blake et al., 2003; Streets and Waldhoff, 1999; Streets et al., 2003; de Gouw et al., 2004; Bertschi et al., 2004]. The sources of these atmospheric constituents are both natural and anthropogenic. For example, fossil fuel and biofuel burning and natural and human-caused biomass fires are significant sources of CO, VOCs and NO<sub>x</sub> in the troposphere. In addition, O<sub>3</sub> is often produced in significant quantities when CO and VOCs react with hydroxyl radicals in the presence of NO<sub>x</sub> and sunlight.

[3] To complement field observations, several studies have used global chemical transport models (GCTM) to probe the influence of Eurasian emissions on the chemical composition of the North American troposphere [Bernsten et al., 1999; Jacob et al., 1999; Fiore et al., 2002, 2003;

<sup>1</sup>Also at Department of Atmospheric Sciences, University of Washington, Seattle, Washington, USA.

Jaeglé *et al.*, 2003; Liu *et al.*, 2003; Liang *et al.*, 2004]. Notably, the GCTM studies indicate that the LRT of urban and industrial pollution from Asia to North America peaks in the spring (March–April) and has less impact in the summer due to climatological factors in Asia and the North Pacific [Merrill *et al.*, 1985, 1989; Hoell *et al.*, 1997; Jacob *et al.*, 1999; Newell and Evans, 2000; Kotchenruther *et al.*, 2001a; Liu *et al.*, 2003; Liang *et al.*, 2004]. For example, using a 3-D GCTM, Jacob *et al.* [1999] report that a tripling of annual Asian anthropogenic NO<sub>x</sub> emissions between 1985 and 2010 will increase mean surface O<sub>3</sub> levels during spring in the western and eastern United States by 2–6 ppbv and 1–3 ppbv, respectively. Jacob *et al.* [1999] note that such an increase will offset the benefits of domestic emissions reductions in the United States with a greater impact during spring than in the summer.

[4] Until now, there have been few observations of the long-range transport of Eurasian emissions to the NE Pacific during the summer. Since 1997, the University of Washington's Photochemical Ozone Budget of the Eastern North Pacific Atmosphere (PHOBEA) science initiative has explored the influence of long-range transport of Eurasian emissions on the chemical composition of the NE Pacific atmosphere using ground-based and airborne observations [Jaffe *et al.*, 2001, 2003a; Kotchenruther *et al.*, 2001a, 2001b; Price *et al.*, 2003, 2004; Jaeglé *et al.*, 2003; Weiss-Penzias *et al.*, 2003, 2004; Bertschi *et al.*, 2004; Liang *et al.*, 2004]. Most of the PHOBEA campaigns were conducted from March through May, although some ground-based measurements lasted throughout summer and fall. For instance, in 2001 ground-based measurements were made in northwestern Washington state at the Cheeka Peak Observatory (CPO) for a full year [Jaffe *et al.*, 2001, 2003a]. Additionally, three PHOBEA airborne campaigns were conducted during the springs of 1999 [Kotchenruther *et al.*, 2001a], 2001 [Price *et al.*, 2003], and 2002 [Bertschi *et al.*, 2004] when vertical profiles of trace gases and aerosols were collected from the surface up to 6 km during the 2001 and 2002 studies and 8 km during the 1999 study.

[5] An important finding from the 2002 study was the influence of Asian boreal fire emissions on the composition of the NE Pacific troposphere during mid-May [Bertschi *et al.*, 2004]. Building on the results of the prior PHOBEA studies, the primary goals of this study included the determination of background concentrations of O<sub>3</sub>, CO and aerosols in the NE Pacific troposphere and whether or not there is evidence of significant LRT events to the NE Pacific during the summer. Other goals, contingent on the identification of LRT events, included characterizing the O<sub>3</sub>-CO-aerosol relationships in LRT plumes and identifying the primary sources of LRT events using our observations coupled with auxiliary models and satellite data. Recently, we have reported that substantial burning in Siberia during the summer of 2003 resulted in the highest seasonal mean concentrations of CO and O<sub>3</sub> ever recorded at 10 ground-based sites located in Alaska, Canada and the northwestern United States [Jaffe *et al.*, 2004]. This paper complements these findings, and to the best of our knowledge, these are the first detailed reports of the episodic transport of Siberian

fire plumes to the northwestern United States during the summer (mid May–August).

## 2. Experiment

[6] Vertical profiles of CO, O<sub>3</sub>, and aerosol scattering of light were collected during 9 flights from 27 May through 5 August 2003 over the region bounded by 47.5°–48.5°N latitude and 124.0°–125.5°W longitude. Our airborne platform has been described in detail elsewhere [Price *et al.*, 2003; Snow *et al.*, 2003; Bertschi *et al.*, 2004] and therefore only a brief description is given here. Simultaneous observations were made at CPO, located at 48.2°N, 124.8°W, and ~500 m above mean sea level (asl), where continuous measurements of a suite of trace gases and particles were made. Weiss-Penzias *et al.* [2003, 2004, and references therein] provide descriptions of the instrumental methods employed at CPO.

### 2.1. Airborne Measurements

[7] The research flights were conducted using a Beechcraft Duchess 76 aircraft, which is flown unpressurized and has a maximum ceiling height of 6 km with a 300 kg payload. All flights originated from Paine Field in Everett, Washington, and consisted of (1) an ascending leg to ~6 km (asl) en route to the Pacific Coast, (2) a spiraling descent from 6 to ~0.1 km for collecting vertical profiles, and (3) a return leg at 1–2 km for a total flight time of ~3 hours. Two rear-facing 3/4 inch o.d. (3/16 inch i.d.) stainless steel inlets were used for continuous sampling of O<sub>3</sub>, CO, and total aerosol scattering of light ( $\sigma_{sp}$ ). In addition, we measured pressure, temperature, relative humidity (RH), and flight coordinates.

[8] Ozone measurements were made using a miniature ultraviolet (UV) absorption analyzer (2B Technologies, Inc. [Bognar and Birks, 1996]) and an electrochemical concentration cell (ECC) ozonesonde (EN-SCI Corp., Model 4Z). The UV absorption O<sub>3</sub> monitor has a precision and accuracy of  $\pm 4$  ppbv for 10 s signal averages and the ECC sonde has a precision and accuracy of  $\pm 2$  ppbv. On the basis of laboratory tests, the response times of the UV absorption and ECC instruments are ~20 s and ~50 s, respectively. Prior to this study, the stainless steel inlet and Teflon tubing used in the O<sub>3</sub> sampling system was tested in our laboratory for O<sub>3</sub> losses and passivation effects. At the sample system flow rate of ~15–20 L min<sup>-1</sup>, no measurable O<sub>3</sub> losses or passivation effects occurred in the stainless steel inlet or Teflon tubing. During flight 4, the UV ozone monitor displayed spurious measurements associated with water interferences, similar to those described by Meyer *et al.* [1991] and Snow *et al.* [2003]. During flights 1–3 no water vapor interferences in the UV absorption measurements were evident and we found an excellent agreement between the ground-based observations made at CPO and the airborne measurements collected at the same elevation. After flight 4, the ozone monitor optics were cleaned to reduce water vapor interferences, however, the ozone monitor continued to have intermittent noise problems coincident with significant variations in RH. Therefore the UV ozone data is used in our analysis of flights 1–3 and the ECC sonde ozone data is used in our analysis of flights 4 through 9.

[9] An integrating nephelometer (TSI, Inc., Model 3563) measured aerosol total scattering coefficients of blue, green, and red light ( $\sigma_{sp}$  (450 nm),  $\sigma_{sp}$  (550 nm), and  $\sigma_{sp}$  (700 nm)), respectively. In prior studies it was determined that particles with a geometric diameter  $>0.8 \pm 0.2 \mu\text{m}$  are excluded from our aerosol scattering measurements due to the flow rates and design of the rear-facing inlet [Price *et al.*, 2003]. The scattering coefficients were corrected to standard temperature and pressure, STP, and are reported as such throughout the remainder of this paper. Nephelometer data were not collected during flight 5 due to a software problem.

[10] An ultraviolet resonance-fluorescence (UV-RF) CO analyzer (Aerolaser, Inc., Model 5002) collected 1 s measurements of CO [Gerbig *et al.*, 1996, 1999]. During each flight, at least two in-flight calibrations were performed using a commercial CO standard in synthetic air (Scott Gas, Inc.), which was referenced to a primary laboratory CO standard (National Institute of Standards and Technology standard reference material, NIST-SRM), similar to our previous methods [Bertschi *et al.*, 2004].

[11] A hand-held Global Positioning System (Trimble, Inc.) was used to log altitude, latitude, and longitude at a frequency of 1 Hz. Ambient temperature and relative humidity measurements were made using a Vaisala, Inc., model HMP45 temperature and RH probe, which extended  $\sim 20$  cm from the outer skin of the aircraft. We compared our temperature and relative humidity vertical profiles with corresponding radiosonde measurements taken over Quilayute, Washington, located  $\sim 50$  km southeast of CPO (available from The University of Wyoming's Department of Meteorology at <http://weather.uwyo.edu/upperair/sounding.html>) and there was an excellent agreement between our temperature and RH vertical profiles and the radiosonde observations.

## 2.2. Auxiliary Observations and Models

[12] Several forecasting tools were employed to aid in the identification of NE Pacific background air. This includes times when regional radiosonde measurements and meteorological forecasts indicated westerly Pacific onshore flows throughout most of the lower troposphere (0–6 km) along the Washington State coast. For postmission analysis, we used a number of modeling databases and satellite observations to aid in the determination of source regions of LRT events.

[13] Three-dimensional back trajectories were calculated using the National Oceanic and Atmospheric Administration, Air Resources Laboratory Hysplit (Hybrid Single-Particle Lagrangian Integrated Trajectory) model [Draxler and Hess, 1997; Draxler, 2003]. Hysplit uses a 3-D vertical velocity model input coupled with the National Center for Environmental Prediction's FNL meteorological data. We used the Hysplit simulations to calculate 10 day back trajectories at 500 m height intervals within the 0–6 km column and closest to the hour when each vertical profile was collected. Additional back trajectories were calculated for the discrete altitudes where air masses of interest were observed. To complement the back trajectories, we investigated the meteorological patterns over the North Pacific throughout the summer of 2003

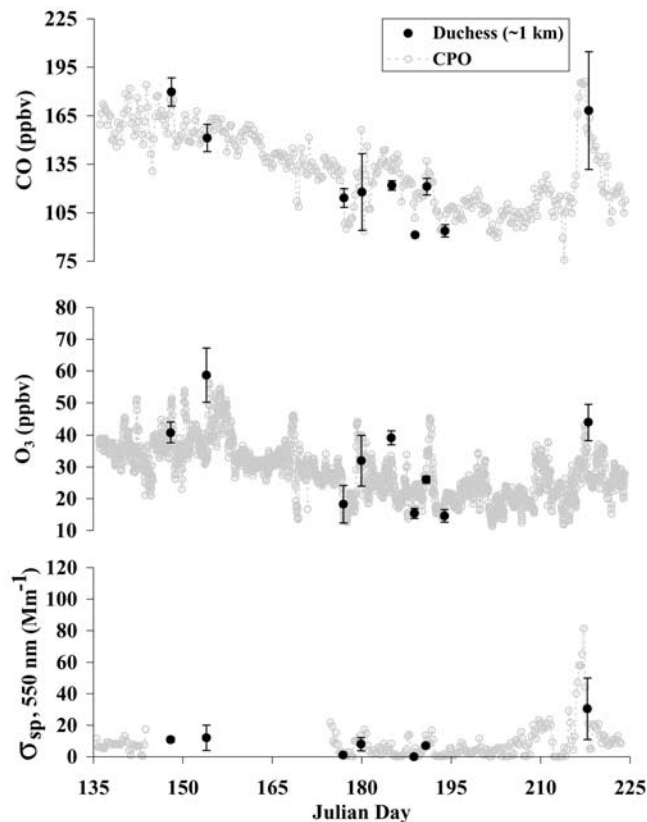


**Figure 1.** Comparison of the summer 2003 airborne observations with ground-based measurements of  $\text{O}_3$ , CO, and  $\sigma_{sp}$  (550 nm) collected between 15 May and 13 August 2003 (Julian days 135–225) at Cheeka Peak Observatory (CPO). The airborne data are the means of the 0–1 km measurements, and the error bars represent the variability ( $1\sigma$ ). During flight 8, Julian day 193, the Duchess was confined to altitudes above 1 km, and the 1–2 km means are plotted instead for this flight. The CPO aerosol and CO observations are 8 hour averages, and the  $\text{O}_3$  observations are 1 hour averages for a better temporal resolution. CPO aerosol scattering measurements were not made from Julian day 144 to 175 (24 May to 24 June).

that influenced transport pathways using climate data from NOAA and the Cooperative Institute for Research in Environmental Sciences Climate Diagnostics Center, <http://www.cdc.noaa.gov>.

[14] To investigate biomass burning activities in Asia during the study period, we analyzed data collected by the Moderate Resolution Imaging Spectroradiometer (MODIS) on board the NASA Terra and Aqua satellites, which detects global fire activity within a  $1^\circ \times 1^\circ$  grid. In our analysis of LRT of aerosols, we used global aerosol optical depth observations made by the NASA Total Ozone Mapping Spectrometer (TOMS, <http://toms.gsfc.nasa.gov>) and the Naval Research Laboratory Aerosol Analysis and Prediction System coupled with global meteorological fields from the Naval Operational Global Atmospheric Prediction System (NAAPS/

**Table 1.** Overview of the Summer 2003 Observations of O<sub>3</sub>, CO, and Total Aerosol Scattering of Light ( $\lambda = 550$  nm,  $\sigma_{sp(550\text{ nm})}$ )<sup>a</sup>

Altitude, km	Flight																		All Airborne 2003		
	1	2	3	4	5	6	7	8	9	Mean	Median	1 $\sigma$									
	<i>O<sub>3</sub>, ppbv</i>																				
5–6	90 (7)	97 (5)	61 (9)	52 (5)	73 (3)	71 (2)	35 (3)	62 (7)	47 (2)	65	62	20									
4–5	73 (3)	98 (5)	60 (5)	37 (6)	72 (6)	66 (2)	19 (7)	66 (3)	51 (5)	60	66	23									
3–4	60 (6)	86 (9)	46 (4)	33 (1)	67 (22)	65 (4)	27 (6)	50 (14)	43 (2)	53	50	18									
2–3	65 (8)	79 (7)	41 (4)	36 (3)	41 (3)	54 (8)	33 (12)	33 (9)	50 (10)	48	41	16									
1–2	45 (8)	82 (15)	46 (6)	27 (3)	36 (5)	38 (10)	37 (6)	15 (2)	60 (10)	43	38	19									
0–1	41 (3)	59 (9)	18 (6)	32 (8)	39 (2)	15 (2)	26 (1)	-	44 (6)	34	36	14									
	<i>CO, ppbv</i>																				
5–6	115 (5)	159 (6)	88 (6)	85 (10)	129 (6)	148 (5)	84 (2)	101 (5)	75 (6)	109	101	30									
4–5	118 (11)	200 (23)	87 (6)	76 (2)	126 (6)	138 (5)	76 (3)	109 (3)	73 (5)	112	109	41									
3–4	120 (5)	171 (16)	87 (5)	75 (4)	110 (18)	118 (7)	85 (4)	107 (9)	83 (6)	106	107	29									
2–3	158 (9)	153 (14)	97 (7)	77 (5)	103 (2)	113 (7)	93 (12)	100 (6)	116 (27)	112	103	27									
1–2	180 (8)	174 (19)	124 (14)	83 (4)	120 (9)	108 (7)	111 (8)	94 (4)	154 (39)	125	120	31									
0–1	(9)	151 (8)	114 (6)	118 (24)	122 (3)	91 (1)	121 (5)	-	168 (36)	133	122	30									
	<i><math>\sigma_{sp(550\text{ nm})}</math>, Mm<sup>-1</sup></i>																				
5–6	5.6 (2.3)	7.4 (2.7)	0.3 (.8)	1.0 (1.0)	-	2.3 (.5)	0 (.7)	1.0 (.7)	0 (1.2)	2.2	1.0	2.8									
4–5	4.2 (2.6)	78.1 (27.5)	1.0 (.8)	0.5 (.7)	-	1.7 (.5)	0 (.7)	1.6 (.6)	0.3 (.9)	10.9	1.3	27.2									
3–4	3.9 (2.0)	35.5 (14.5)	1.3 (.8)	0.4 (.6)	-	1.4 (.6)	0 (.5)	1.7 (1.2)	1.9 (1.4)	5.8	1.6	12.1									
2–3	21.4 (10.3)	22.9 (10.2)	1.6 (1.2)	0.6 (.6)	-	2.2 (1.1)	1.4 (1.9)	1.4 (.8)	6.3 (5.4)	7.2	1.9	9.4									
1–2	12.3 (3.4)	51.9 (24.1)	5.5 (4.6)	1.7 (.8)	-	2.6 (1.3)	4.5 (2.9)	0 (.2)	14.4 (8.0)	11.6	5.0	17.1									
0–1	12.2 (4.0)	14.6 (10.2)	1.4 (1.7)	7.5 (4.5)	-	0 (.3)	8.6 (1.7)	-	37.5 (24.3)	11.7	8.6	12.5									

<sup>a</sup>The data represent the mean and 1 standard deviation of the mean ( $1\sigma$ , in parentheses) for 1 km binned data. Also provided are the binned means, medians, and  $1\sigma$  of the binned flight data. The Julian days for flights 1–9 are 148, 154, 177, 180, 185, 189, 191, 194, and 218 respectively. The flight dates for flights 1–9 are 27 May 2003, 2 June 2003, 25 June 2003, 28 June 2003, 3 July 2003, 7 July 2003, 9 July 2003, 12 July 2003, and 5 August 2003, respectively.

NOGAPS) [Hogan and Rosmond, 1991; Hogan and Brady, 1993; Reid *et al.*, 2004].

### 3. Results and Discussion

#### 3.1. Overview of the Summer 2003 Airborne and Ground-Based Observations

[15] Table 1 provides a statistical summary of all the flight data collected in this study and Figure 1 shows the Duchess observations of the 0–1 km average CO, O<sub>3</sub>, and aerosol scattering on the nine flights compared with the continuous CPO data. There are two notable features in the boundary layer data shown in Figure 1. First is the large enhancement of O<sub>3</sub>, CO and aerosol concentrations during several periods throughout the 2003 summer. Notably, on 3–6 August, hourly-average concentrations of CO, O<sub>3</sub> and aerosol scattering exceeded 220 ppbv, 58 ppbv, and 110 Mm<sup>-1</sup>, respectively. This period had the highest aerosol scattering levels ever recorded at CPO. Figure 1 shows that the aircraft observations were made during the latter period of this event. A second, subtler feature is the relatively high background levels of CO in the early summer. For example, from 15 May through 30 June the median CO concentration at CPO was 150 ppbv. During this same period in 2001, the CPO median CO mixing ratio was 111 ppbv. The enhanced summer background CO was corroborated by similar observations made at several sites located in Alaska, Canada, and the Pacific Northwest United States during the summer of 2003 [Jaffe *et al.*, 2004]. Two important findings of the study by Jaffe *et al.* [2004] are (1) over the past decade, there has been a good correlation between the annual area burned during the Russian fire season and mean summer CO and O<sub>3</sub> mixing ratios at 10 sites in northwestern North America and (2) the large area burned during the 2003

Russian fire season led to unprecedented enhancements in summer background CO and O<sub>3</sub> concentrations over northwestern North America.

#### 3.2. Case Studies of Summer 2003 LRT Events

[16] During 27 May, 2 June, and 5 August 2003, the Duchess platform sampled three significant LRT events. In all of these cases, we observed highly correlated layers of O<sub>3</sub>, CO, and aerosols within the 0–6 km column. Back trajectories indicate that all of the LRT events originated from westerly Asian continental outflow 6 to >10 days before arriving to North America. For our analysis we use criteria adapted from our previous airborne study to define what constitutes a LRT event [Bertschi *et al.*, 2004]. First, using our 1 s measurement data, both CO and total aerosol scattering of green light (“ $\sigma_{sp(550\text{ nm})}$ ” or “tsg”) must be elevated relative to monthly or seasonal median levels by >50 ppbv and 20 Mm<sup>-1</sup>, respectively. Second, local winds must be consistently from the Pacific and away from regional pollution sources for the duration of the event. Finally, air mass back trajectories must be consistent with the local winds and indicate trans-Pacific transport.

##### 3.2.1. Flight 1: 27 May 2003

[17] Figure 2a shows the O<sub>3</sub>, CO, and  $\sigma_{sp(550\text{ nm})}$  vertical profiles collected from ~2200 to 2230 UTC during flight 1 and includes the 2003 median vertical profiles from all 9 flights for comparison. During this flight, meteorological conditions at the sampling location were mostly clear with a band of clouds from ~3.5 to 3 km. A polluted layer of air was located directly below the cloud band and extended down to 1.7 km where O<sub>3</sub>, CO and  $\sigma_{sp(550\text{ nm})}$  surpassed 75 ppbv, 170 ppbv, and 35 Mm<sup>-1</sup>, respectively. Figure 2a also shows a distinct layer of pollution directly below the upper pollution band located between 1.7 km and the

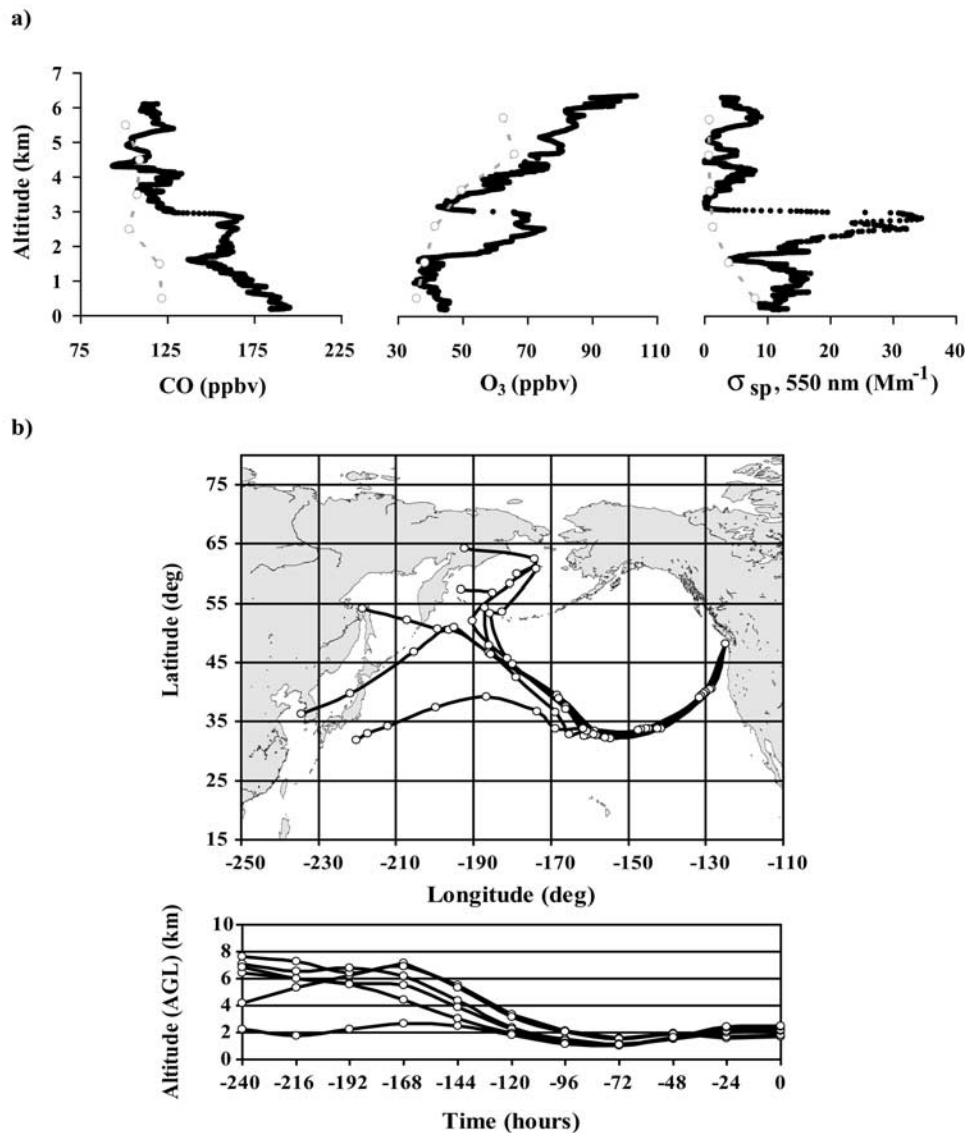


**Figure 2.** (a) Vertical profiles of O<sub>3</sub>, CO, and  $\sigma_{sp}$  (550 nm) collected from ~2200–2230 UTC during 27 May event. Also shown are the summer 2003 kilometer-binned median vertical profiles (circles and dashed line) for comparison. (b) Ten day Hysplit back trajectories and time-height profiles for the 1.7 to 2.8 km layer of the 27 May event. The back trajectories were initialized at 200 m intervals within the 1.7–2.8 km layer over 48.2°N, 124.8°W at 2200 UTC, 27 May 2003.

surface. Relative to the campaign median vertical profiles, the O<sub>3</sub> and aerosol scattering enhancements were not as large in the lower pollution layer compared to the enhancements in the upper layer. In contrast, CO mixing ratios were larger in the lower pollution layer than the upper layer. Meteorological observations made over Quillayute, Washington, and at CPO indicated that surface winds were from the south and east, suggesting that the lower pollution band may have contained pollutants from North American anthropogenic sources. However, the Quillayute radiosonde measurements indicate that westerly and southwesterly winds were prevalent above 1 km. Furthermore; the Hysplit model indicates the 1.7–2.7 km layer did not pass over North America prior to its arrival over CPO.

[18] Figure 2b shows the 10-day Hysplit back trajectories and time-height profiles at 100 m intervals from 1.7 to 2.8 km over the sample area (48.2°N, 124.8°W) on 27 May 2003 at 2200 UTC. The back trajectories originate over a vast region of far east Asia (between 45° and 65°N latitude) and, coupled with NOAA/CDC data for 15 May to 27 May, indicate that the westerly Asian continental outflow between 2 and 8 km above ground level (agl) was transported southeastward toward the central North Pacific as a result of the anticyclonic circulation of a high-pressure system centered near ~25°–35°N, 160°–170°E. Before arriving in North America, another high-pressure system off the southern California coastline (30°–40°N, 130°–140°W) coupled with the cyclonic rotation of the Aleutian low conducted

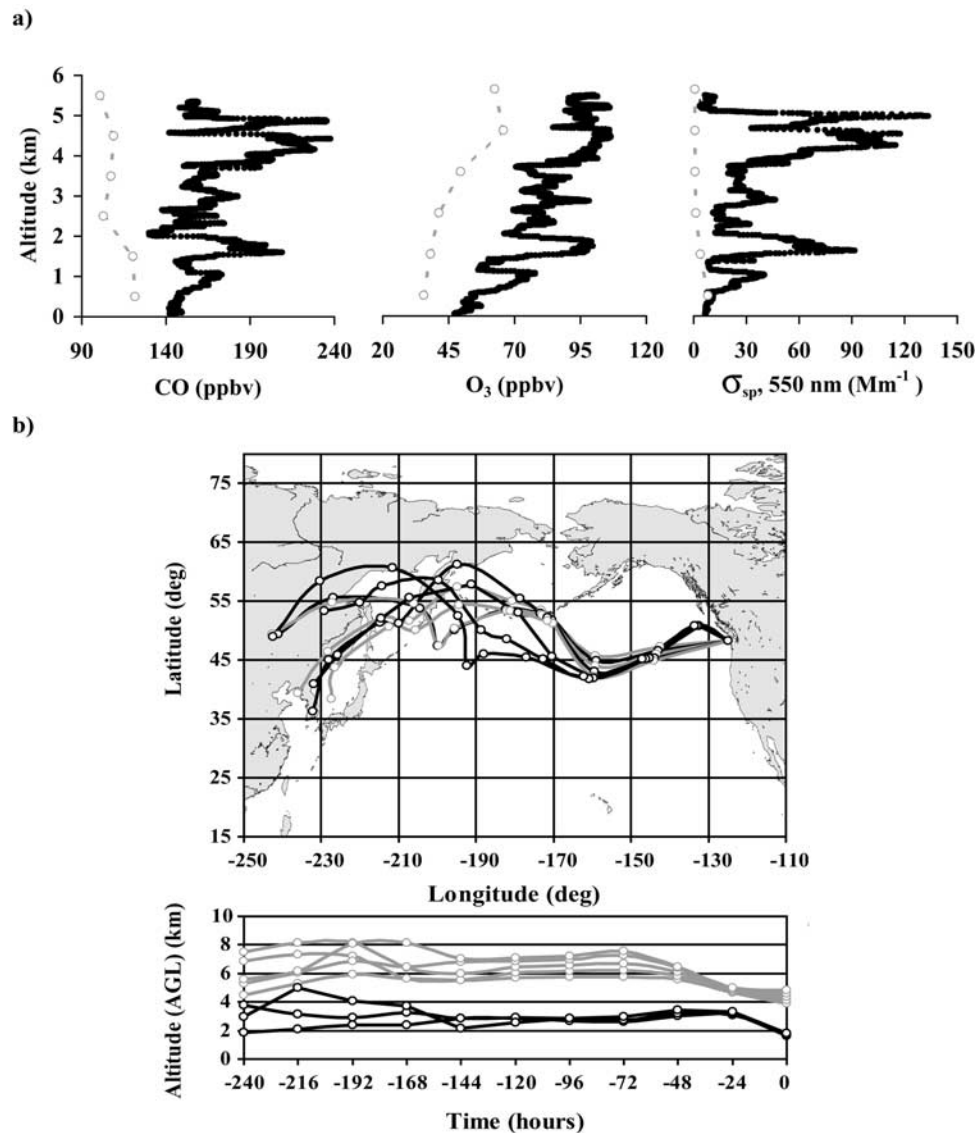


**Figure 3.** Same as Figure 2, but showing (a) the vertical profiles collected during the 2 June event and (b) the 10 day Hysplit back trajectories and time-height profiles for the 1.5–2.0 km and 3.8–4.9 km layers. The back trajectories were initialized at  $\sim 200$  m intervals within the 1.7–2.8 km layer over  $48.2^{\circ}\text{N}$ ,  $124.8^{\circ}\text{W}$  at 2200 UTC, 2 June 2003.

this air mass to the northeast where it first crossed over the U.S. coastline near CPO.

### 3.2.2. Flight 2: 2 June 2003

[19] Figure 3a shows the vertical profiles from the LRT event observed during 2 June 2003. During this flight O<sub>3</sub>, CO and aerosol enhancements were widespread throughout the 0–6 km column. The two layers with the largest enhancements were observed between  $\sim 1.5$  and 2.0 km and 3.8 and 5.0 km. Both of these layers contained O<sub>3</sub> and CO mixing ratios exceeding 95 and 200 ppbv, respectively, and accounted for the highest aerosol scattering values ( $\sim 104$  and  $141 \text{ Mm}^{-1}$ , respectively) observed throughout the history of the PHOBEA airborne campaigns [Kotchenruther *et al.*, 2001a; Price *et al.*, 2003; Bertschi *et al.*, 2004].

[20] Figure 3b illustrates the Hysplit back trajectories for the 1.5–2.0 km (solid) and 3.8–5.0 km (shaded) layers on 2 June 2003 at 2200 UTC. Similar to the 27 May event, the Hysplit model indicates that the air masses originated from the area bounded by  $35^{\circ}$ – $60^{\circ}\text{N}$  latitude and  $120^{\circ}$ – $150^{\circ}\text{E}$  longitude and traversed the Pacific in  $\sim 7$  to 10 days. Between the transport times of the 2 June and 27 May events, the Aleutian Low shifted northward to  $\sim 55^{\circ}$ – $60^{\circ}\text{N}$ ,  $160^{\circ}$ – $165^{\circ}\text{W}$ . The influence of the Aleutian Low and a Pacific high-pressure system at  $\sim 25^{\circ}$ – $35^{\circ}\text{N}$ ,  $170^{\circ}$ – $180^{\circ}\text{W}$  brought the air masses eastward toward North America. Thus, in contrast with the 27 May event, the 2 June event trajectory paths remained above  $40^{\circ}\text{N}$  latitude and traveled a more direct route to Washington State. The 2 June 2003 Quillayute radiosonde indicated westerly and northwesterly

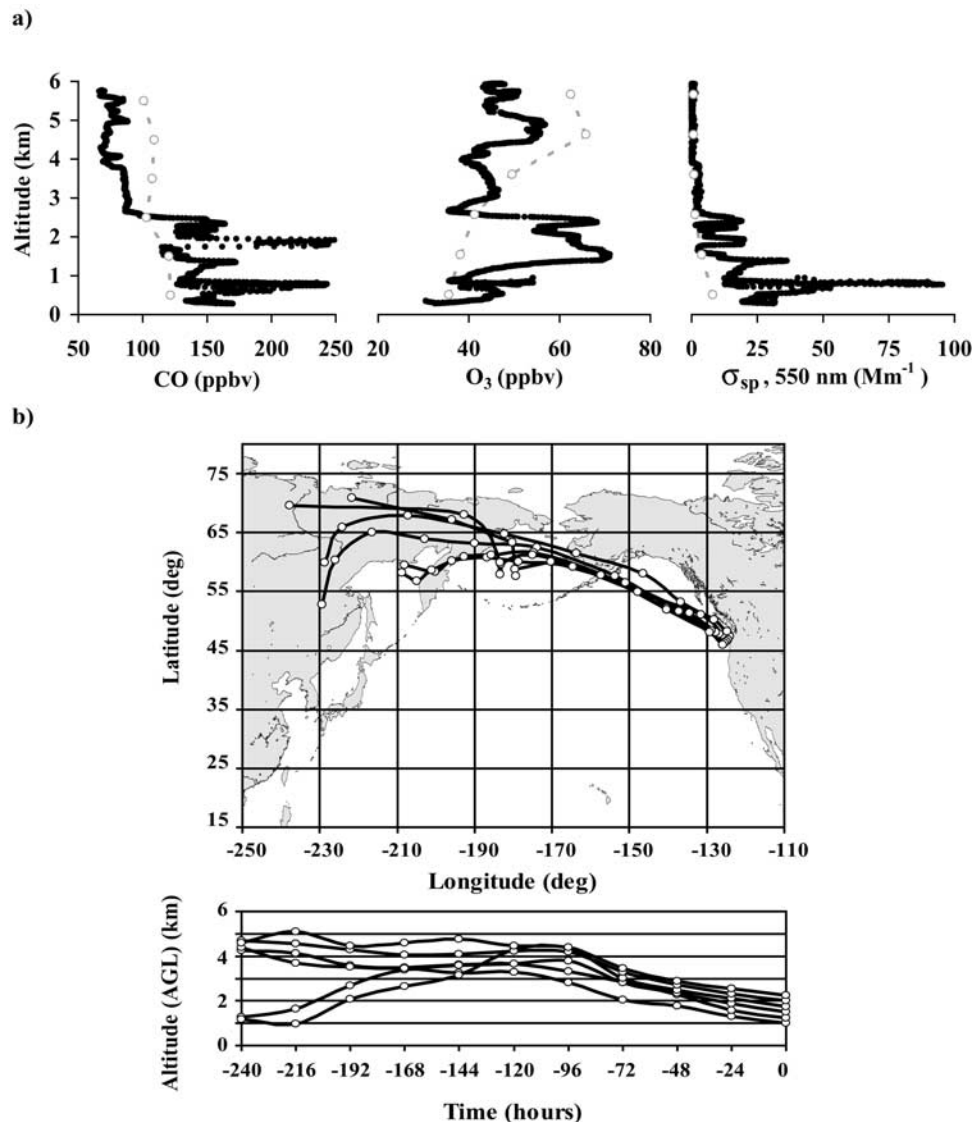


**Figure 4.** Same as Figure 2, but showing (a) the vertical profiles collected during the 5 August event and (b) the 10 day Hysplit back trajectories and time-height profiles for the 1.0–2.2 km column at 2000 UTC, 5 August 2003.

winds throughout the 0–6 km column, corroborating the Hysplit back-trajectory paths.

### 3.2.3. Flight 9: 5 August 2003

[21] Figure 4a shows the vertical profiles collected during flight 9. Meteorological conditions were mostly clear skies with southwesterly winds throughout the 0–6 km column. The air masses below 2.5 km contained many fine structured layers (<100 m thick) containing O<sub>3</sub>, CO and aerosol enhancements. The 5 August observations illustrate the advantage of the faster response times of the CO and aerosol scattering instruments compared to that of the ECC ozone-sonde (see section 2.1). The CO and aerosol scattering vertical profiles show multiple layers of polluted air masses interspersed between relatively clean air masses below 2.5 km, which led to a wide range in the observed CO and  $\sigma_{sp}$  (550 nm) levels ( $\sim$ 100 to 200 ppbv and 5 to 100 Mm<sup>-1</sup>, respectively) within the 1 and 2 km binned data (Table 1). A polluted layer at  $\sim$ 2 km accounted for the

highest concentrations of CO, yet aerosol scattering in this layer was relatively low.

[22] Figure 4b shows the Hysplit 10 day back trajectories for the layers located between  $\sim$ 1.0 and 2.2 km during 5 August 2003 at 2000 UTC. The 10 day back trajectories indicate that this event originated over eastern Siberia (north of  $\sim$ 55°N latitude and west of  $\sim$ 125°E) at altitudes varying from 1 to 5 km above ground level (agl). According to NOAA/CDC reanalysis data, a high-pressure system located over the Sea of Okhotsk ( $\sim$ 55°N, 150°E) prevented the westerly outflow of this air mass from crossing south of 55°N. Thus the Asian westerly outflow was transported over the Siberian Peninsula to the Bering Sea between a high-pressure system in the central North Pacific ( $\sim$ 45°N, 170°W) and a low-pressure system over the interior of Alaska ( $\sim$ 65°–70°N, 130°–140°W) brought the event to the Gulf of Alaska. According to the Hysplit model, the event had a cumulative trans-Pacific transport time of  $\sim$ 6–

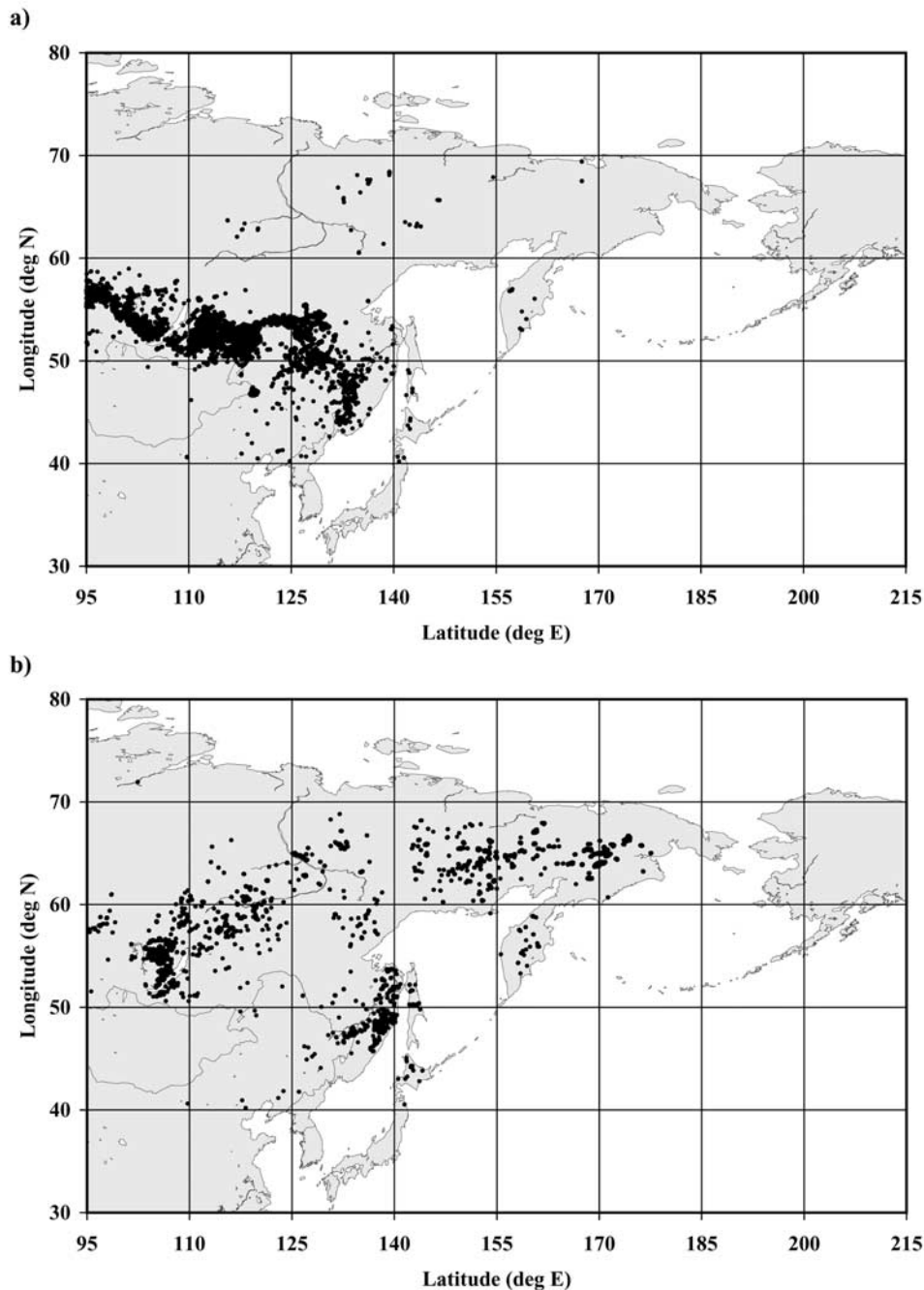


**Figure 5.** NASA Terra and Aqua Moderate Resolution Imaging Spectroradiometer (MODIS) fire detections in northeast Asia from (a) 15 to 25 May and (b) 21 to 31 July 2003. Each point represents the center of a  $1 \times 1$  km pixel that has been flagged as containing one or more actively burning fires within that pixel.

7 days. The time-height profiles in Figure 4b indicate that this air mass subsided from 5 km to 1 km approximately 2 to 3 days before its arrival. As noted above, observations made at CPO indicate the presence of this event over northwestern Washington State from 3 to 6 August and indicated that the airborne observations were made during the latter period of this multiday event.

[23] The polluted layers interspersed with cleaner layers of air shown in Figure 4a suggest that the cleaner layers may come from significantly different source regions. However, the trajectories in Figure 4b indicate that these

cleaner air masses came from the same source region. Additional trajectories were calculated at 300 m altitude intervals from 0.5 to 2.1 km (ASL) at the four corners of a  $1 \times 1$  degree grid centered around the vertical profiling location. The trajectories above 0.9 km showed no evidence that the air masses originated from a different source region.

### 3.3. Sources of the Events: Indicators of LRT of Siberian Biomass Fire Emissions

[24] The correlated  $O_3$ , CO, and aerosol enhancements coupled with the Hysplit back trajectories suggest origins

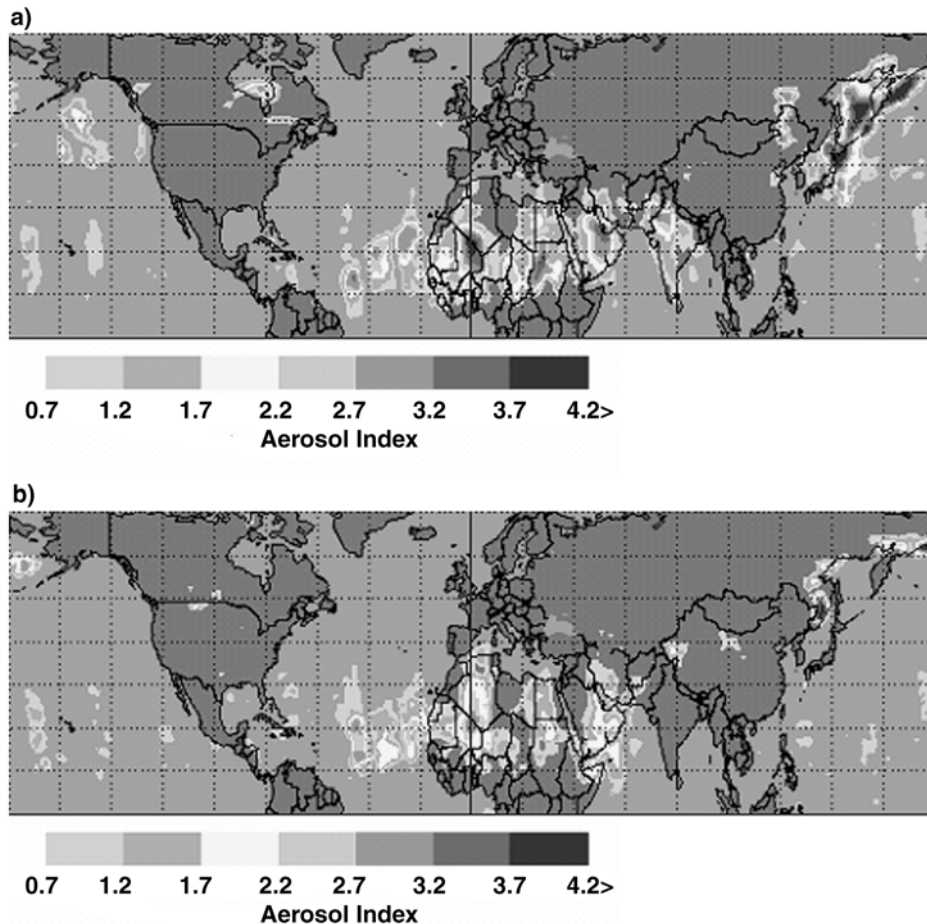


**Figure 6.** NASA Total Ozone Mapping Spectrometer (TOMS) global aerosol index data for (a) 24 May and (b) 27 July 2003. The images indicate westerly transport of smoke over the North Pacific Ocean and are consistent with the back trajectories shown in Figures 2–4. See color version of this figure at back of this issue.

from combustion sources within Asia. Several field studies have reported that transported Asian plumes may contain a complex mixture of trace gas and particle emissions from multiple combustion sources [Oberlander *et al.*, 2002; Jacob *et al.*, 2003; Blake *et al.*, 2003; Li *et al.*, 2003; de Gouw *et al.*, 2004; Bertschi *et al.*, 2004] and, under certain circumstances, may also be composed of significant amounts of mineral dust [Jaffe *et al.*, 2003a, 2003b; Price *et al.*, 2003; Husar *et al.*, 2001; McKendry *et al.*, 2001; VanCuren and Cahill, 2002; VanCuren, 2003]. Because the events originated over a vast area of urban, agricultural, desert and forest subregions, windborne dust and industrial/urban emissions may have contributed to the events to some degree. However, several indicators suggest that a major source of the events was the much larger than normal 2003 Russian boreal fire season.

[25] According to reports from the Global Fire Monitoring Center, GFMC ([www.fire.uni-freiburg.de](http://www.fire.uni-freiburg.de)), widespread biomass fires burned in the Siberian boreal zone throughout the summer of 2003, with the most intense burning periods during May–early June and August. On the basis of AVHRR satellite data analysis, the GFMC estimates that ~18.9 million ha burned during the 2003 Russian fire season. For comparison, several studies indicate that, on

average, ~8 to 10 million ha burn each year in the Russian boreal forests, but with considerable interannual variability [Conard and Ivanova, 1997; Goldammer and Stocks, 2000; Kasischke *et al.*, 1999; Cahoon *et al.*, 1994, 1996; Sukhinin *et al.*, 2003]. As noted, Jaffe *et al.* [2004] report the relationship between the annual Russian area burned and background O<sub>3</sub> and CO concentrations in western North America and include a case study of the influence that the LRT of Russian biomass burning emissions had on enhancements in surface O<sub>3</sub> concentrations in western North America.

[26] Figure 5 depicts the NASA MODIS fire detections in northeast Asia from 15 to 25 May (Figure 5a) and 21 to 31 July 2003 (Figure 5b). Figure 5a shows that throughout May 2003 a large number of fires were detected along the Russian borders with Mongolia and China between 45° and 60°N, with the highest fire activity east of Lake Baikal. Figure 5b shows sustained fire activity in the regions near Lake Baikal, but indicates a higher level of fire activity in northeastern Russia north of 60°N. This seasonal pattern is likely due to decreasing fuel moisture throughout June and July in the Arctic climates allowing for surface fuels to dry out sufficiently and sustain combustion.

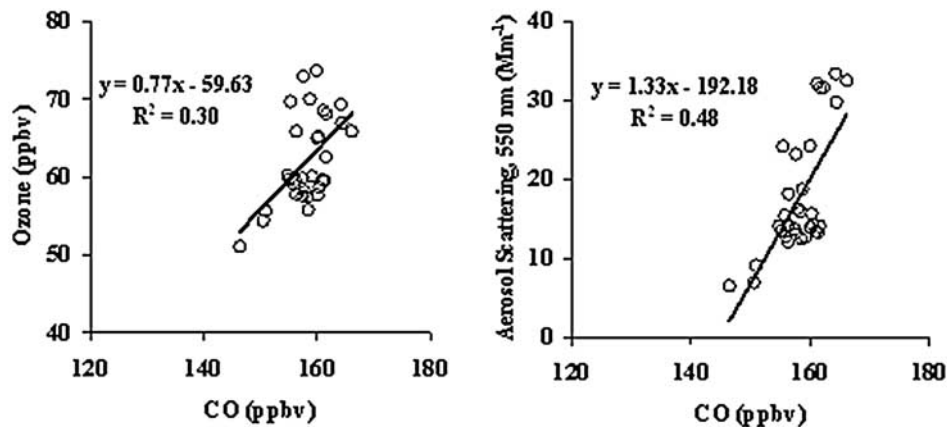


**Figure 7.** Plots of  $O_3$  versus CO and  $\sigma_{sp}$  ( $550\text{ nm}$ ) versus CO for the 3.0–1.7 km layer of the 27 May event. The slopes of the least squares linear regressions provide an estimate of the  $O_3/CO$  and  $\sigma_{sp}$  ( $550\text{ nm}$ )/CO ERs, respectively.

[27] While the MODIS fire detections established intense fire activity occurring in these regions, the NASA TOMS data indicates the transport of aerosols from Siberia to the Pacific. For example, Figure 6 shows the NASA TOMS aerosol index for 24 May (Figure 6a) and 27 July (Figure 6b) 2003. Figure 6a shows a massive aerosol plume carried over the Sea of Okhotsk and the Bering Sea during late May. Also shown are substantial aerosol plumes located over the Gulf of Alaska. Similarly, Figure 6b indicates large plumes of smoke were transported from northeastern Siberia to the Bering Sea during late July. The locations of the large smoke plumes shown in Figure 6a are consistent with the paths of the back trajectories in Figures 2 and 3, and those shown in Figure 6b are consistent with the trajectories in Figure 4. In addition, the NAAPS/NOGAPS model supports the dominance of smoke and dust in the observed plumes, which are discussed in greater detail by Jaffe *et al.* [2004].

### 3.4. Enhancement Ratios of the Summer 2003 Events

[28] The difference between the CO concentrations in a polluted air mass from that of the CO concentrations in the background air ( $\Delta CO = CO_{\text{pollution}} - CO_{\text{bkg}}$ ) can be used to normalize the excess mixing ratio of a coemitted species (i.e.,  $\Delta X/\Delta CO$ ). Because CO is indicative of combustion sources and has a relatively long tropospheric lifetime,  $\Delta O_3/\Delta CO$  (called the enhancement ratio or “ $O_3/CO$  ER”) is

commonly used as an indicator of photochemical  $O_3$  production in polluted air masses originating from combustion processes [Wofsy *et al.*, 1992; Jacob *et al.*, 1992; Parrish *et al.*, 1993; Mauzerall *et al.*, 1996; Goode *et al.*, 2000; Forster *et al.*, 2001; Price *et al.*, 2004; Bertschi *et al.*, 2004]. Because the determination of background concentrations of CO and trace gases can present difficulties, we used two methods to determine the  $O_3/CO$  ERs. Our first method uses the background  $O_3$  and CO concentrations, inferred by the layers above and below the polluted layer. The second method uses the slope of the linear fit of the  $O_3$  versus CO scatterplot. Figure 7 shows an example of the second method used for the 3.0–1.7 km layer of the 27 May event. In our measurements of the 5 August event, the difference in the response times of the  $O_3$  and CO monitors made the use of the second technique impractical, and therefore only the first method was used to determine the  $O_3/CO$  ER for this case.

[29] Table 2 gives the layer averaged  $O_3/CO$  and  $\sigma_{sp}$  ( $550\text{ nm}$ )/CO ERs for the three 2003 events and, for comparison, provides  $O_3/CO$  ERs from five previous reports of LRT of boreal fire emissions to middle and high northern latitudes [Bertschi *et al.*, 2004; Forster *et al.*, 2001; Wotawa and Trainer, 2000; McKeen *et al.*, 2002; Mauzerall *et al.*, 1996; Wofsy *et al.*, 1992]. With the exception of the PHOBEA studies, all of these studies describe the transport

**Table 2.**  $O_3/CO$  and  $\sigma_{sp}$  ( $550\text{ nm}$ )/CO Enhancement Ratios of the 2003 Events and From Previous Studies of LRT of Boreal Smoke to Middle and High Northern Latitudes<sup>a</sup>

Source	Year	Date	Location of Observations	Plume Height, km	$\Delta O_3/\Delta CO$ , ppbv ppbv <sup>-1</sup>	$\sigma_{sp}$ ( $550\text{ nm}$ )/ $\Delta CO$ , Mm <sup>-1</sup> ppbv <sup>-1</sup>
This study	2003	27 May	NE Pacific/NW United States	1.5–3.0	0.84 (0.37)	1.10 (0.45)
This study	2003	2 June	NE Pacific/NW United States	1.0–2.5	0.64 (0.22)	0.99 (0.31)
				3.5–5.0	0.37 (0.19)	1.24 (0.41)
This study	2003	5 August	NE Pacific/NW United States	0.7–1.2	0.15 (0.04)	0.84 (0.17)
				1.7–2.0	0.19 (0.05)	0.24 (0.05)
Bertschi <i>et al.</i> [2004]	2002	14–23 May	NE Pacific/NW United States	3.5–5.5	0.22–0.36	0.51–0.99
Forster <i>et al.</i> [2001]	1998	05–11 Aug.	Western Europe	3.0–6.0	0.3	n.r.
Wotawa and Trainer [2000]	1995	10 July	South central United States	1.5–3.0	0.11	n.r.
McKeen <i>et al.</i> [2002]		07 July	Nashville, Tennessee	0.0–1.5	0.17	n.r.
Mauzerall <i>et al.</i> [1996]	1990	21 July to 15 Aug.	Canada	2.0–4.0	0–0.66	n.r.
Wofsy <i>et al.</i> [1992]	1988	26 July to 03 Aug.	Alaska	2.0–4.5	0.04–0.18	n.r.

<sup>a</sup>Uncertainty is reported in parentheses. Here “n.r.” is not reported in study.

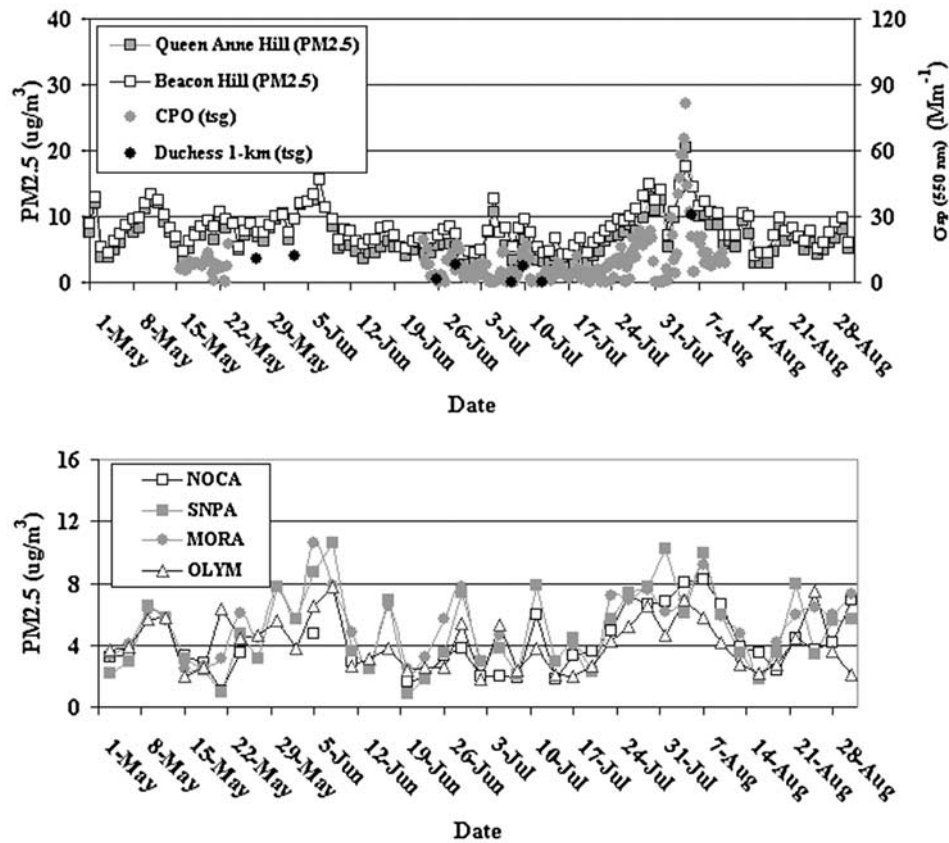


**Figure 8.** Temporal profiles of aerosol concentrations and total scattering ( $\lambda = 550 \text{ nm}$ ) in northwestern Washington State during 2003. Twenty-four hour average  $\text{PM}_{2.5}$  concentrations (in  $\mu\text{g m}^{-3}$ ) are reported for monitoring stations in (top) Seattle, Washington, and (bottom) IMPROVE monitoring networks. For comparison the CPO and Duchess 1 km total scattering observations (in  $\text{Mm}^{-1}$ ) are overlaid with the Seattle  $\text{PM}_{2.5}$  observations. The IMPROVE sites are North Cascades (NOCA,  $48.7^\circ\text{N}$ ,  $121.1^\circ\text{W}$ , 576 m), Snoqualmie Pass (SNPA,  $47.4^\circ\text{N}$ ,  $121.4^\circ\text{W}$ , 1160 m), Mount Rainier (MORA,  $46.8^\circ\text{N}$ ,  $122.1^\circ\text{W}$ , 427 m), and Olympic (OLYM,  $48.0^\circ\text{N}$ ,  $123.0^\circ\text{W}$ , 600 m).

of North American boreal forest fire smoke [Wofsy *et al.*, 1992; Mauzerall *et al.*, 1996; Wotawa and Trainer, 2000; McKeen *et al.*, 2002; Forster *et al.*, 2001]. The  $\text{O}_3/\text{CO}$  ERs observed during 27 May and 2 June in this study are relatively high. Although Mauzerall *et al.* [1996] report  $\text{O}_3/\text{CO}$  ERs as high as  $0.66 \text{ ppbv ppbv}^{-1}$ , they provide a mean  $\text{O}_3/\text{CO}$  ER of  $0.1 \pm 0.2 \text{ ppbv ppbv}^{-1}$  in aged boreal smoke due to undetectable  $\text{O}_3$  enhancements in five out of nine plumes. Several possibilities for our higher  $\text{O}_3/\text{CO}$  ERs in Table 2 include atmospheric mixing during transit, losses of CO due to reaction with OH, efficient net  $\text{O}_3$  production at the source, and/or slower rates of  $\text{O}_3$  loss during transport. For example, the production and eventual decomposition of peroxyacetyl nitrate, PAN, in aged boreal fire emissions may reduce  $\text{O}_3$  loss rates during transit [Jacob *et al.*, 1992].

[30] With the exception of the 1.7–2.0 km layer of the 5 August event, the total aerosol scattering enhancement ratios,  $\sigma_{\text{sp}}(550 \text{ nm})/\text{CO}$  ERs, surpassed  $0.84 \text{ Mm}^{-1} \text{ ppbv}^{-1}$ . This is comparable with the  $\sigma_{\text{sp}}(550 \text{ nm})/\text{CO}$  ERs observed in the May biomass burning events of our 2002 study ( $0.51$ – $0.99 \text{ Mm}^{-1} \text{ ppbv}^{-1}$ ) [Bertschi *et al.*, 2004] and consistent with high aerosol emission rates (relative to CO) reported for large fire plumes [Ward and Hardy, 1991; FIRESCAN

Science Team, 1996]. Possibilities for the low  $\sigma_{\text{sp}}(550 \text{ nm})/\text{CO}$  ERs during the 5 August event include low particle emissions at the source and/or dry and wet deposition during transit. To investigate the latter possibility, we used the Hysplit model to compute rainfall rates for the event trajectories. For the 5 August 1.8–2.0 km layer, the Hysplit precipitation model indicated that a total of 18–25 mm of rain fell through the air mass represented by the back trajectories. During transit of the 2 June and 27 May events, the Hysplit model indicated relatively low rainfall rates, with 10 day rainfall totals  $<12 \text{ mm}$ . This suggests that there could have been a higher fraction of aerosols scavenged due to precipitation during transport of the 5 August event compared to that of the first two events.

### 3.5. Influence of Boreal Smoke on North American Surface Air Quality

[31] For the case of 6 June 2003, Jaffe *et al.* [2004] report that  $\text{O}_3$  concentrations at Enumclaw, Washington, exceeded the U.S. EPA 8 hour  $\text{O}_3$  standard ( $0.08 \text{ ppmv}$ ) [U.S. Environmental Protection Agency, 2000] and estimate that the LRT of Siberian smoke accounted for  $\sim 15 \text{ ppbv}$  of the maximum  $96 \text{ ppbv}$   $\text{O}_3$  (8 hour average) observed at this site.

The 2 June airborne observations corroborate these observations as significant amounts of aerosols were transported with  $O_3$  in the lower troposphere (0–6 km). Figure 8 shows 24 hour average  $PM_{2.5}$  concentrations from 1 May through 31 August measured at Puget Sound Clean Air Agency (PSCAA) stations in Seattle, Washington, and the CPO and Duchess 1 km aerosol measurements (Figure 8, top) and  $PM_{2.5}$  concentrations measured at Interagency Monitoring of Protected Visual Environments (IMPROVE) sampling stations at remote sites in northwestern Washington State (Figure 8, bottom). During the summer of 2003, the Seattle  $PM_{2.5}$  concentrations typically varied from 3 to  $10 \mu\text{g m}^{-3}$ , mostly due to local sources such as transportation and industries. Notably, the highest  $PM_{2.5}$  concentrations were measured during the first weeks of June and August, coinciding with the 2 June and 5 August events. Peak 24 hour average concentrations of  $\sim 16$  and  $20 \mu\text{g m}^{-3}$  were observed in Seattle on 7 June and 5 August, respectively. The June 2003  $PM_{2.5}$  maximum concentrations correspond to a buildup of  $PM_{2.5}$  concentrations from 2–7 June and mimic the daily  $O_3$  trends described by Jaffe *et al.* [2004]. The 2 June event was the largest observed during our airborne campaign (ground-based aerosol observations were unavailable at CPO during this period). However,  $PM_{2.5}$  concentrations at the IMPROVE sites were enhanced by  $\sim 5 \mu\text{g m}^{-3}$  from 5 to 8 June.

[32] Figure 8 shows a second period of enhanced  $PM_{2.5}$  concentrations throughout northwestern Washington State from 30 July to 7 August. Peak 24 hour average concentrations in Seattle exceeded  $18 \mu\text{g m}^{-3}$  and led to a “moderate” U.S. EPA Air Quality Index rating (51). This episode also coincided with our airborne and ground-based aerosol observations as total aerosol scattering levels at CPO exceeded  $50 \text{ Mm}^{-1}$  from 3–4 August. Assuming a mass-scattering efficiency,  $\alpha_s(550\text{nm})$ , of  $\sim 3 \pm 2 \text{ m}^2 \mu\text{g}^{-1}$  for aged smoke aerosols [Reid *et al.*, 1998], we make a conservative estimate that the CPO aerosol scattering observations account for 24 hour  $PM_{2.5}$  concentrations of 8– $10 \mu\text{g m}^{-3}$ , which is consistent with the  $PM_{2.5}$  enhancements in Seattle and at the IMPROVE sites during this event. These observations indicate that there was a nonlocal source of aerosols in Seattle, which contributed a significant fraction of the enhanced pollutant concentrations during the June and August LRT events.

#### 4. Conclusions

[33] We used airborne and ground-based measurements to investigate the chemical composition of the 0–6 km column of the NE Pacific during the summer of 2003. To the best of our knowledge, this study is the first to report several distinct episodes of LRT of Siberian smoke plumes to northwestern North America during the summer (May–August). Coincident to our summer campaign, an estimated 18.9 million hectares burned during the Siberian boreal fire season, which accounted for the largest Russian area burned in comparison to recent fire seasons. Our airborne observations, coupled with satellite data and global atmospheric transport simulations, indicate that the 2003 Siberian fires played an important role in shaping the chemical and aerosol properties of the NE Pacific troposphere.

[34] The observations of Siberian smoke plumes indicate that these events are associated with the efficient transport and production of  $O_3$ . In addition to  $O_3$ , relatively high aerosol mass loading was observed in the plumes as indicated by relatively high  $\sigma_{\text{sp}}(550 \text{ nm})/\text{CO}$  ERs. This is consistent with previous observations of high particle emission rates from large biomass fires. While the  $\sigma_{\text{sp}}(550 \text{ nm})/\text{CO}$  ERs may be useful for identifying the LRT of biomass fire emissions, it is susceptible to factors such as low particle emission rates at the source and/or deposition processes during transport. Significant precipitation scavenging was determined to be a possible cause of the low  $\sigma_{\text{sp}}(550 \text{ nm})/\text{CO}$  ER ( $< 0.25 \text{ Mm}^{-1} \text{ ppbv}^{-1}$ ) observed during the 5 August event. Finally, two events coincided with episodes of air quality degradation in the Puget Sound Region of Washington state. The LRT event sources, added to local sources, raised pollutant concentrations to environmentally significant levels in both of these case studies.

[35] The case studies of summertime long-range transport presented in this paper complement prior springtime research intensives (PEM-West A and B, ACE-Asia, BIBLE 2000, TRACE-P, ITCT 2002, PHOBEA 99, 2001, 2002), which established that Asian anthropogenic and natural emission sources have a significant impact on background pollutant levels in North America. However, the majority of these prior studies focused primarily on the springtime (late February through early May) LRT of Asian emissions. This study, and the report by Jaffe *et al.* [2004], show that high-latitude Asian emissions also play an important role in shaping the chemical composition of the northwestern North American troposphere during the summer, which is when North American  $O_3$  air quality problems are most acute. This likely reflects the northward shift of the Pacific High and transport pathways during late spring and summer [Zhao *et al.*, 2003].

[36] Jaffe *et al.* [2004] indicate that the mean annual area burned during the Russian Boreal fire season has increased throughout the past decade. Similarly, Kasischke *et al.* [1999] report that the average, annual area burned in North American boreal forests has more than doubled in the past 30 years, corresponding with an increase in average, annual temperatures in this region. This suggests that the average annual area burned in the global Boreal zone will likely continue to increase in response to current trends in global climate change. Therefore it is pertinent that measurement and modeling studies of LRT consider the dynamics of boreal forest fires to improve our understanding of atmospheric chemistry with respect to global climate change.

[37] **Acknowledgments.** We gladly acknowledge James Dennison and Jon Hiller for their technical and clerical support throughout this research. We would like to acknowledge Suresh Kumar and Diane Davies at the University of Maryland for providing NASA Terra/MODIS and Aqua/MODIS data for the fire maps used in this work. We also wish to thank Doug Westphal, Jeffery Reid and the Naval Academy Research Laboratory (NARL) for providing information pertaining to the NAAPS/NOGAPS simulations used in this study. Finally, we commend Jim Grant and the pilots of Northway Aviation for their professionalism and flying expertise. This research was supported by funds provided by the National Science Foundation.

#### References

- Andreae, M. O., H. Berresheim, T. W. Andreae, M. A. Kritz, T. S. Bates, and J. T. Merrill (1988), Vertical distribution of dimethylsulfide, sulfur dioxide, aerosol ions, and radon over the northeast Pacific Ocean, *J. Atmos. Chem.*, *6*, 149–173.

- Bernsten, T. K., S. Karlsdottir, and D. A. Jaffe (1999), Influence of Asian emissions on the composition of air reaching the north western United States, *Geophys. Res. Lett.*, *26*, 2171–2174.
- Bertschi, I. T., D. A. Jaffe, L. Jaeglé, H. U. Price, and J. B. Dennison (2004), PHOBEA/ITCT 2002 airborne observations of transpacific transport of ozone, CO, volatile organic compounds, and aerosols to the northeast Pacific: Impacts of Asian anthropogenic and Siberian boreal fire emissions, *J. Geophys. Res.*, *109*, D23S12, doi:10.1029/2003JD004328.
- Bey, I., D. J. Jacob, J. A. Logan, and R. M. Yantosca (2001), Asian chemical outflow to the Pacific: Origins, pathways and budgets, *J. Geophys. Res.*, *106*, 23,097–23,114.
- Blake, N. J., et al. (2003), NMHCs and halocarbons in Asian continental outflow during the Transport and Chemical Evolution over the Pacific (TRACE-P) Field Campaign: Comparison with PEM-West B, *J. Geophys. Res.*, *108*(D20), 8806, doi:10.1029/2002JD003367.
- Bognar, J. A., and J. W. Birks (1996), Miniaturized ultraviolet ozonesonde for atmospheric measurements, *Anal. Chem.*, *68*, 3059–3062.
- Cahoon, D. R., Jr., B. J. Stocks, J. S. Levine, W. R. Cofer II, and J. M. Pierson (1994), Satellite analysis of the severe 1987 forest fires in northern China and southeastern Siberia, *J. Geophys. Res.*, *99*, 18,627–18,638.
- Cahoon, D. R., Jr., B. J. Stocks, J. S. Levine, W. R. Cofer III, and J. A. Barber (1996), Monitoring the 1992 forest fires in the boreal ecosystem using NOAA AVHRR satellite imagery, in *Biomass Burning and Global Change*, edited by J. S. Levine, pp. 795–801, MIT Press, Cambridge, Mass.
- Conard, S. G., and G. A. Ivanova (1997), Wildfire in Russian boreal forests—Potential impacts of fire regime characteristics on emissions and global carbon balance estimates, *Environ. Pollut.*, *98*, 305–313.
- de Gouw, J. A., et al. (2004), Chemical composition of air masses transported from Asia to the U. S. West Coast during ITCT 2K2: Fossil fuel combustion versus biomass-burning signatures, *J. Geophys. Res.*, *109*, D23S20, doi:10.1029/2003JD004202.
- Draxler, R. R. (2003), Evaluation of an ensemble dispersion application, *J. Appl. Meteorol.*, *42*, 308–317.
- Draxler, R. R., and G. D. Hess (1997), Description of the Hysplit 4 modeling system, *Tech Memo ERL ARL-224*, NOAA, Silver Spring, Md., Dec.
- Fiore, A. M., D. J. Jacob, I. Bey, R. M. Yantosca, B. D. Field, and A. C. Fusco (2002), Background ozone over the United States in summer: Origin, trend, and contribution to pollution episodes, *J. Geophys. Res.*, *107*(D15), 4275, doi:10.1029/2001JD000982.
- Fiore, A., D. J. Jacob, H. Liu, R. M. Yantosca, T. D. Fairlie, and Q. Li (2003), Variability in surface ozone background over the United States: Implications for air quality policy, *J. Geophys. Res.*, *108*(D24), 4787, doi:10.1029/2003JD003855.
- FIRESCAN Science Team (1996), Fire in ecosystems of boreal Eurasia: The Bor forest island fire experiment fire research campaign Asia-North (FIRESCAN), in *Biomass Burning and Global Change*, edited by J. S. Levine, pp. 848–873, MIT Press, Cambridge, Mass.
- Forster, C., et al. (2001), Transport of boreal forest fire emissions from Canada to Europe, *J. Geophys. Res.*, *106*, 22,887–22,906.
- Gerbig, C., D. Kley, A. Volz-Thomas, J. Kent, K. Dewey, and D. S. McKenna (1996), Fast response resonance fluorescence CO measurements aboard the C-130: Instrument characterization and measurements made during North Atlantic Regional Experiment 1993, *J. Geophys. Res.*, *101*, 29,229–29,238.
- Gerbig, C., S. Schmitgen, D. Kley, A. Volz-Thomas, K. Dewey, and D. Haaks (1999), An improved fast-response vacuum-UV resonance fluorescence CO instrument, *J. Geophys. Res.*, *104*, 1699–1704.
- Goldammer, J. G., and B. J. Stocks (2000), Eurasian perspective of fire: Dimension, management, policies, and scientific requirements, in *Fire, Climate Change, and Carbon Cycling in the Boreal Forest*, edited by E. S. Kasischke and B. J. Stocks, pp. 49–65, Springer, New York.
- Goode, J. G., R. J. Yokelson, D. E. Ward, R. A. Susott, R. E. Babbitt, M. A. Davies, and W. M. Hao (2000), Measurements of excess O<sub>3</sub>, CO<sub>2</sub>, CO, CH<sub>4</sub>, C<sub>2</sub>H<sub>4</sub>, C<sub>2</sub>H<sub>2</sub>, HCN, NO, NH<sub>3</sub>, HCOOH, CH<sub>3</sub>COOH, HCHO, and CH<sub>3</sub>OH in 1997 Alaskan biomass burning plumes by airborne Fourier transform infrared spectroscopy (AFTIR), *J. Geophys. Res.*, *105*, 22,147–22,166.
- Hoell, J. M., D. D. Davis, S. C. Liu, R. E. Newell, H. Akimoto, R. J. McNeal, and R. J. Bendura (1997), The Pacific Explorer Mission—West Phase B: February–March, 1994, *J. Geophys. Res.*, *102*, 28,223–28,239.
- Hogan, T. F., and L. R. Brady (1993), Sensitivity studies of the Navy's global forecast model parameterizations and evaluation of improvements to NOGAPS, *Mon. Weather Rev.*, *121*, 2373–2395.
- Hogan, T. F., and T. E. Rosmond (1991), The description of the Navy operational global atmospheric prediction system's spectral forecast model, *Mon. Weather Rev.*, *119*, 1786–1815.
- Husar, R. B., et al. (2001), Asian dust events of April 1998, *J. Geophys. Res.*, *106*, 18,317–18,330.
- Jacob, D. J., et al. (1992), Summertime photochemistry of the troposphere at high northern latitudes, *J. Geophys. Res.*, *97*, 16,421–16,431.
- Jacob, D. J., J. A. Logan, and P. P. Murti (1999), Effect of rising Asian emissions on surface ozone in the United States, *Geophys. Res. Lett.*, *26*, 2175–2178.
- Jacob, D. J., J. H. Crawford, M. M. Kleb, V. S. Connors, R. J. Bendura, J. L. Raper, G. W. Sachse, J. C. Grille, L. Emmons, and C. L. Heald (2003), Transport and Chemical Evolution over the Pacific (TRACE-P) aircraft mission: Design, execution, and first results, *J. Geophys. Res.*, *108*(D20), 9000, doi:10.1029/2002JD003276.
- Jaeglé, L., D. Jaffe, H. U. Price, P. Weiss-Penzias, P. I. Palmer, M. J. Evans, D. J. Jacob, and I. Bey (2003), Sources and budgets for CO and O<sub>3</sub> in the northeastern Pacific during the spring of 2001: Results from the PHOBEA-II experiment, *J. Geophys. Res.*, *108*(D20), 8802, doi:10.1029/2002JD003121.
- Jaffe, D. A., et al. (1999), Transport of Asian air pollution to North America, *Geophys. Res. Lett.*, *26*, 711–714.
- Jaffe, D. A., T. Anderson, D. Covert, B. Trost, J. Danielson, W. Simpson, D. Blake, J. Harris, and D. Streets (2001), Observations of ozone and related species in the Northeast Pacific during the PHOBEA campaigns: 1. Ground-based observations at Cheeka Peak, *J. Geophys. Res.*, *106*, 7449–7461.
- Jaffe, D. A., I. MacKendry, T. Anderson, and H. Price (2003a), Six “new” episodes of trans-Pacific transport of air pollutants, *Atmos. Environ.*, *37*, 391–404.
- Jaffe, D., J. Snow, and O. Cooper (2003b), The April 2001 Asian dust events: Transport and substantial impact on surface particulate matter concentrations across the United States, *EOS trans.*, *84*(46), pp. 501, 507.
- Jaffe, D., I. Bertschi, L. Jaeglé, P. Novelli, J. S. Reid, H. Tanimoto, R. Vingarzan, and D. Westphal (2004), Long-range transport of Siberian biomass burning emissions and impact on surface ozone in western North America, *Geophys. Res. Lett.*, *31*, L16106, doi:10.1029/2004GL020093.
- Kasischke, E. S., K. Bergen, R. Fennimore, F. Sotelo, G. Stephens, A. Janetos, and H. H. Shugart (1999), Satellite imagery gives a clear picture of Russia's boreal forest fires, *Eos Trans. AGU*, *80*, 141, 147.
- Kotchenruther, R. A., D. A. Jaffe, H. J. Beine, T. L. Anderson, J. W. Bottenheim, J. M. Harris, D. R. Blake, and R. Schmitt (2001a), Observations of ozone and related species in the northeast Pacific during the PHOBEA campaigns: 2. Airborne observations, *J. Geophys. Res.*, *106*, 7463–7483.
- Kotchenruther, R. A., D. A. Jaffe, and L. Jaeglé (2001b), Ozone photochemistry and the role of peroxyacetyl nitrate in the springtime northeastern Pacific troposphere: Results from the Photochemical Ozone Budget of the Eastern North Pacific Atmosphere (PHOBEA) campaign, *J. Geophys. Res.*, *106*, 28,731–28,742.
- Kritz, M. A., J. C. LeRouley, and E. F. Danielsen (1990), The China Clipper—Fast advective transport of radon-rich air from the Asian boundary layer to the upper troposphere near California, *Tellus, Ser. B*, *42*, 46–61.
- Li, Q., D. J. Jacob, R. M. Yantosca, C. L. Heald, H. B. Singh, M. Koike, Y. Zhao, G. W. Sachse, and D. G. Streets (2003), A global three-dimensional model analysis of the atmospheric budgets of HCN and CH<sub>3</sub>CN: Constraints from aircraft and ground measurements, *J. Geophys. Res.*, *108*(D21), 8827, doi:10.1029/2002JD003075.
- Liang, Q., L. Jaeglé, D. A. Jaffe, P. Weiss-Penzias, A. Heckman, and J. A. Snow (2004), Long-range transport of Asian pollution to the northeast Pacific: Seasonal variations and transport pathways of carbon monoxide, *J. Geophys. Res.*, *109*, D23S07, doi:10.1029/2003JD004402.
- Liu, H., D. J. Jacob, I. Bey, R. M. Yantosca, B. N. Duncan, and G. W. Sachse (2003), Transport pathways for Asian pollution outflow over the Pacific: Interannual and seasonal variations, *J. Geophys. Res.*, *108*(D20), 8786, doi:10.1029/2002JD003102.
- Mauzerall, D. L., D. J. Jacob, S. M. Fan, J. D. Bradshaw, G. L. Gregory, G. W. Sachse, and D. R. Blake (1996), Origin of tropospheric ozone at remote high northern latitudes in summer, *J. Geophys. Res.*, *101*, 4175–4188.
- McKeen, S. A., et al. (2002), Ozone production from Canadian wildfires during June and July of 1995, *J. Geophys. Res.*, *107*(D14), 4192, doi:10.1029/2001JD000697.
- McKendry, I. G., J. P. Hacker, R. Stull, S. Sakiyama, D. Mignacca, and K. Reid (2001), Long-range transport of Asian dust to the Lower Fraser Valley, British Columbia, Canada, *J. Geophys. Res.*, *106*, 18,361–18,370.
- Merrill, J. T., R. Bleck, and L. Avila (1985), Modeling atmospheric transport to the Marshall Islands, *J. Geophys. Res.*, *90*, 12,972–12,936.
- Merrill, J. T., M. Uematsu, and R. Bleck (1989), Meteorological analysis of long range transport of mineral aerosol over the North Pacific, *J. Geophys. Res.*, *94*, 8584–8598.

- Meyer, C. P., C. M. Elsworth, and I. E. Galbally (1991), Water vapor interference in the measurement of ozone in ambient air by ultraviolet absorption, *Rev. Sci. Instrum.*, *62*(1), 223–228.
- Newell, R. E., and E. J. Evans (2000), Seasonal changes in pollutant transport to the North Pacific: The relative importance of Asian and European sources, *Geophys. Res. Lett.*, *27*, 2509–2512.
- Oberlander, E. A., et al. (2002), Trace gas measurements along the Trans-Siberian railroad: The TROICA 5 expedition, *J. Geophys. Res.*, *107*(D14), 4206, doi:10.1029/2001JD000953.
- Parrish, D. D., C. J. Hahn, E. J. Williams, R. B. Norton, F. C. Fehsenfeld, H. B. Singh, J. D. Shetter, B. W. Gandrud, and B. A. Ridley (1992), Indication of photochemical histories of Pacific air masses from measurements of atmospheric trace species at Point Arena, California, *J. Geophys. Res.*, *97*, 15,883–15,901.
- Parrish, D. D., J. S. Holloway, M. Trainer, P. C. Murphy, G. L. Forbes, and F. C. Fehsenfeld (1993), Export of North American ozone pollution to the North Atlantic Ocean, *Science*, *259*, 1436–1439.
- Price, H. U., D. A. Jaffe, P. V. Doskey, I. McKendry, and T. L. Anderson (2003), Vertical profiles of O<sub>3</sub>, aerosols, CO and NMHCs in the northeast Pacific during the TRACE-P and ACE-ASIA experiments, *J. Geophys. Res.*, *108*(D20), 8799, doi:10.1029/2002JD002930.
- Price, H. U., D. A. Jaffe, O. R. Cooper, and P. V. Doskey (2004), Photochemistry, ozone production, and dilution during long-range transport episodes from Eurasia to the northwest United States, *J. Geophys. Res.*, *109*, D23S13, doi:10.1029/2003JD004400.
- Reid, J. S., P. V. Hobbs, R. J. Ferek, D. R. Blake, J. V. Martins, M. R. Dunlap, and C. Lioussé (1998), Physical, chemical, and optical properties of regional hazes dominated by smoke in Brazil, *J. Geophys. Res.*, *103*, 32,059–32,080.
- Reid, J. S., E. M. Prins, D. L. Westphal, C. C. Schmidt, K. A. Richardson, S. A. Christopher, T. F. Eck, E. A. Reid, C. A. Curtis, and J. P. Hoffman (2004), Real-time monitoring of South American smoke particle emissions and transport using a coupled remote sensing/box-model approach, *Geophys. Res. Lett.*, *31*, L06107, doi:10.1029/2003GL018845.
- Snow, J. A., J. B. Dennison, D. A. Jaffe, H. U. Price, J. K. Vaughan, and B. Lamb (2003), Aircraft and surface observations in Puget Sound and a comparison to a regional model, *Atmos. Environ.*, *37*, 4019–4032.
- Streets, D. G., and S. T. Waldhoff (1999), Present and future emissions of air pollutants in China: SO<sub>2</sub>, NO<sub>x</sub>, and CO, *Atmos. Environ.*, *34*, 363–374.
- Streets, D., et al. (2003), An inventory of gaseous and primary aerosol emissions in Asia in the year 2000, *J. Geophys. Res.*, *108*(D21), 8809, doi:10.1029/2002JD003093.
- Sukhinin, A. I., V. V. Ivanov, E. I. Ponomarev, O. A. Slinkina, A. V. Cherepanov, E. A. Pavlichenko, V. Y. Romansko, and S. I. Miskiv (2003), The 2002 fire season in the Asian part of the Russian Federation, *Int. For. Fire News*, *28*, 1–34.
- U.S. Environmental Protection Agency (2000), National air quality and emission trends report: 1998, *EPA-454/R-00-003*, Research Triangle Park, N. C.
- VanCuren, R. A. (2003), Asian aerosols in North America: Extracting the chemical composition and mass concentration of the Asian continental aerosol plume from long-term aerosol records in the western United States, *J. Geophys. Res.*, *108*(D20), 4623, doi:10.1029/2003JD003459.
- VanCuren, R. A., and T. A. Cahill (2002), Asian aerosols in North America: Frequency and concentration of fine dust, *J. Geophys. Res.*, *107*(D24), 4804, doi:10.1029/2002JD002204.
- Ward, D. E., and C. C. Hardy (1991), Smoke emissions from wildland fires, *Environ. Int.*, *17*, 117–134.
- Weiss-Penzias, P., D. A. Jaffe, A. McClintick, E. M. Prestbo, and M. S. Landis (2003), Gaseous elemental mercury in the marine boundary layer: Evidence for rapid removal in anthropogenic pollution, *Environ. Sci. Technol.*, *37*(17), 3755–3763.
- Weiss-Penzias, P., D. A. Jaffe, A. McClintick, L. Jaeglé, and Q. Liang (2004), Influence of long-range-transported pollution on the annual and diurnal cycles of carbon monoxide and ozone at Cheeka Peak Observatory, *J. Geophys. Res.*, *109*, D23S14, doi:10.1029/2004JD004505.
- Wofsy, S. C., et al. (1992), Atmospheric chemistry in the Arctic and Subarctic: Influence of natural fires, industrial emissions, and stratospheric inputs, *J. Geophys. Res.*, *97*, 16,731–16,746.
- Wotawa, G., and M. Trainer (2000), The influence of Canadian forest fires on pollutant concentrations in the United States, *Science*, *288*, 324–328.
- Zhao, T. L., S. L. Gong, X. Y. Zhang, and I. G. McKendry (2003), Modeled size-segregated wet and dry deposition budgets of soil dust aerosol during ACE-Asia 2001: Implications for trans-Pacific transport, *J. Geophys. Res.*, *108*(D23), 8665, doi:10.1029/2002JD003363.

---

I. T. Bertschi and D. A. Jaffe, Department of Interdisciplinary Arts and Sciences, University of Washington, 18115 Campus Way NE, Bothell, WA 98011, USA. (isaacpb@u.washington.edu)

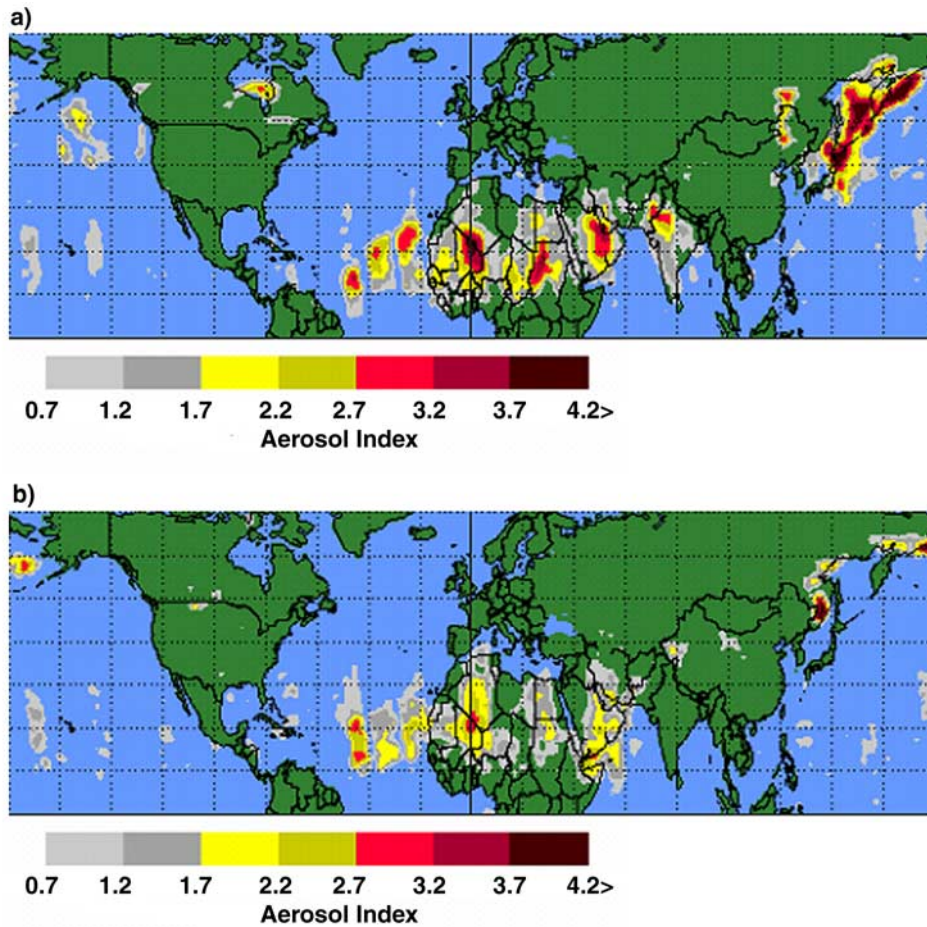


**Figure 6.** NASA Total Ozone Mapping Spectrometer (TOMS) global aerosol index data for (a) 24 May and (b) 27 July 2003. The images indicate westerly transport of smoke over the North Pacific Ocean and are consistent with the back trajectories shown in Figures 2–4.